Materials Transactions, Vol. 54, No. 4 (2013) pp. 466 to 471
Special Issue on Materials-System Integration for Fusion DEMO Blanket

OVERVIEW

Neutron Irradiation Behavior of Tungsten

Akira Hasegawa*[1], Makoto Fukuda*[2], Takashi Tanno*[2,3] and Shuhei Nogami

Department of Quantum Science and Energy Engineering, Faculty of Engineering, Tohoku University, Sendai 980-8579, Japan

Tungsten (W) is a candidate for the plasma facing component material of fusion reactors. During fusion reactor operation, not only displacement damage but also transmutation elements such as rhenium (Re) and osmium (Os) are produced in W by neutron irradiation. To understand the irradiation response of W in a fusion reactor, irradiation effects on hardening, microstructure development and electric resistivity of pure W and W–Re–Os alloys are studied using fission reactor irradiation. In the low-dpa region (<0.4 dpa), irradiation hardening was suppressed by Re addition, but significant hardening appeared in W–26Re alloy after high-dpa (>1 dpa) irradiation. The hardening was caused by the irradiation-induced precipitation of WRe (σ–phase) and WRe_3 (χ–phase). Os was more effective in the irradiation hardening than Re owing to the similar irradiation-induced precipitate formation even in low-dpa region. On the bases of these results, the alloy design of W for fusion reactor applications is suggested. [doi:10.2320/matertrans.MG201208]

(Received October 10, 2012; Accepted January 16, 2013; Published March 1, 2013)

Keywords: *radiation damage, tungsten and tungsten alloys, fusion reactor application, plasma-facing component*

1. Introduction

Since tungsten (W) has a high melting point and a high sputtering resistance to energetic particles, it is considered to be a candidate for the plasma-facing component (PFC) materials of magnetic confinement fusion reactors such as the first wall of a blanket and a diverter plate.[1–3] During fusion reactor operation, as a result of high-energy neutron exposure, not only displacement damage but also transmutation elements are produced. The transmutation elements can be classified into two groups. The first is gas elements such as hydrogen and helium produced by (n, p) or (n, α) reactions. These reactions mainly occur in the high-neutron-energy region above several MeV. The relatively high production rate of these gas atoms by 14 MeV neutron irradiation is characteristic of fusion reactors compared with fission reactors in which the average energy of fission neutrons is approximately 2 MeV. The other is solid elements produced by the by-products of (n, p), (n, α) and (n, γ) reactions. The (n, γ) reactions mainly occur in the low-energy region below 100 keV. PFC will thus be exposed to not only 14 MeV neutrons from the fusion plasma but also low-energy neutrons moderated and backscattered from the blanket, cooling or shielding components of the fusion reactor. The neutron energy spectrum of the low-energy region is strongly dependent on reactor cooling materials such as water, He gas or liquid metals.[4] In general, the characteristic points of transmutation of W in fusion reactors are a low production rate of gas elements and a significant amount of solid elements such as rhenium (Re) and osmium (Os). With increasing neutron irradiation fluence, pure W will change to W–Re–Os–Ta alloys, for example; previous calculations have predicted that pure W will become W–18Re–3Os after 50 dpa irradiation at the first wall.[4]

The predicted amounts of displacement damage and Re content that would be produced in W at the first wall and diverter plate of the ITER and a DEMO-like fusion power reactor were reported by Bolt *et al.*[1] After 5 years of operation in the DEMO-like reactor, the average neutron fluence would be 10 MWa/m^2 at the first wall and 5 MWa/m^2 at the diverter, the displacement damage and Re content would be 30 dpa and 6% in W of the first wall, and 15 dpa and 3% in the diverter, respectively. Operating temperatures are expected to be 500–800°C at the first wall, and 600–1300°C at the diverter, depending on the cooling system used. On the other hand, the calculated helium and hydrogen concentrations in W after 10 MWa/m^2 neutron irradiation were approximately 30 and 60 appm, respectively.[4] In the ITER, a displacement damage of 0.7 dpa and transmutation of 0.15% Re are predicted at the W diverter after a neutron fluence of 0.15 MWa/m^2 at 200–1000°C.

For the application of W to PFC of the diverter and first wall, a radiation-resistant W-based material, which will suffer considerable property degradation caused by the neutron irradiation, is required. To develop the radiation-resistant W-based materials and to predict the material behavior of a component under actual neutron irradiation, a basic understanding of radiation effects in W is also required. The objective of this work is to summarize the irradiation behavior of W from the viewpoint of damage structure development and the effect of transmutation elements based on our previous studies, and to provide insights into future experimental works to develop radiation-resistant PFC-W.

2. Irradiation Conditions and Tested Materials

Between the 1960s and the 1980s, the Experimental Breeder Reactor-II (EBR-II), which was a fast neutron spectrum reactor, was mainly used for studying the irradiation behavior of W in the USA and heavy irradiations up to 10 dpa at higher temperatures were carried out and the results published in a limited number of papers.[5–11] We have been using several experimental reactors, not only in Japan but also in the USA, for W irradiation experiments.[12–21] Figure 1 summarizes the irradiation conditions, temperature and displacement damage in our previous experiments in both published and unfinished studies. The irradiation

*[1]Corresponding author, E-mail: akira.hasegawa@qse.tohoku.ac.jp
*[2]Graduate Student, Tohoku University
*[3]Present address: Japan Atomic Energy Agency, Oarai, Ibaraki 311-1393, Japan

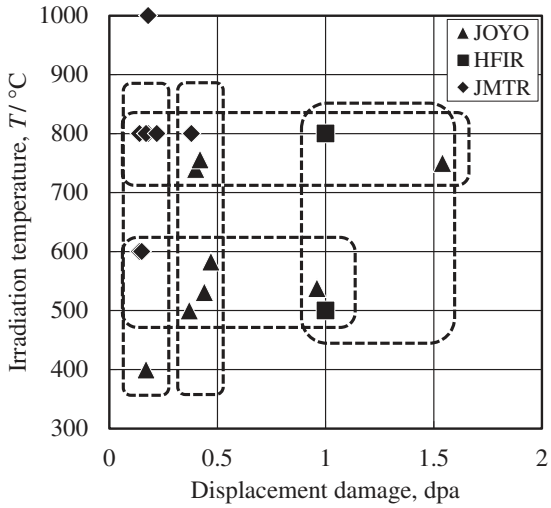

Fig. 1 Irradiation matrix of W and W alloys studied in previous works.[12–21)]

temperatures were classified into two regions, one is the low-temperature region between 400 and 600°C, and the other is the high-temperature region between 750 and 800°C. The Japan Material Testing Reactor (JMTR) and High Flux Isotope Reactor (HFIR) are mixed spectrum reactors, and the amount of nuclear transmutation from W to Re increase even when the dpa was approximately 1. After 1 dpa irradiation in the HFIR, pure W is estimated to transform into W–9Re–5Os alloys. In the case of JMTR irradiation, the dpa level was normally less than 0.15 dpa, and the amount of transmuted Re would be less than 1.8%. In the case of JOYO irradiation, which is a fast experimental reactor in Japan, the amount of Re was estimated to be 1.5% after 1.54 dpa irradiation.[20)]

We have been using two types of W in our works. The first is 0.2 mm-thick hot-rolled sheets of W and W–Re alloys supplied by Plansee Corporation. Standard TEM disk specimens of 3 mm diameter were punched out from the as-received sheets and heat treated at 1300, 1400 or 1600°C for 1 h in vacuum. The aim of this heat treatment was stress relief (SR) at 1300°C and recrystallization (R) at 1600°C. The second set of W was arc-melted (Arc) ingots that we fabricated in collaboration with the Institute of Materials Research (IMR), Tohoku University. TEM disks of 0.2 mm thickness were fabricated from the ingots using electrodischarge machining, and the surfaces were polished using emery papers and annealed at 1400°C for 1 h in vacuum before irradiation. The alloy series of W–xRe–yOs ($x = 0$, 3, 5, 10, 26; $y = 0$, 3, 5) were fabricated.[22)] The compositions of the alloys were in the single-phase region in the W–Re–Os phase diagram at 1600°C.[23)] These specimens were loaded in He or He–Ar gas filled capsules and irradiated in fission reactors.

Hardness tests were carried out using a micro-Vickers test machine using a 200 gf load and a loading time of 30 s at room temperature. Microstructural observations were carried out using a JEM-2010 transmission electron microscope operating at 200 kV. Thin foil specimens for TEM observations were prepared using a twin-jet polishing machine with an electrolyte of 1 mass% NaOH in water. Electrical resistivity measurements were carried out by the four-probe method at 20°C using the specimens of 3 mm diameter and 0.2 mm thickness used for TEM observations.[14)] Before

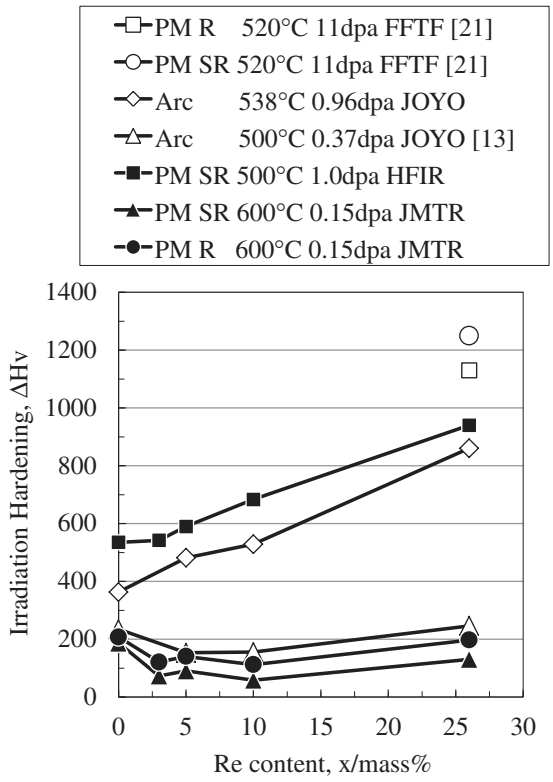

Fig. 2 Irradiation hardening of W and W–Re alloys after neutron irradiation between 500 and 600°C as a function of Re content.[16)]

irradiation, no hardness and electrical resistivity differences between the recrystallized (R) W–xRe alloys and the arc-melted W–xRe alloys were observed in this work.

3. Irradiation Hardening of W and W–Re Alloys

Irradiation hardening of W and W–Re at 500 and 600°C as a function of Re content is shown in Fig. 2.[16)] The data shows that irradiation hardening (ΔHv) of W–Re alloys was less than that of pure W, and the Re concentration dependence of ΔHv was smaller in the low-dpa (<0.37 dpa) region. With increasing fluence to 1 dpa, irradiation hardening became larger and the magnitude of the hardening depended on the Re content. The hardening of W–xRe alloys in HFIR was more than that in JOYO. This may be attributed to the amount of transmutation elements. The production rate of transmutation elements such as Re and Os under HFIR irradiation conditions is 7 to 10 times higher than that under JOYO irradiation conditions owing to the large amount of thermal neutron flux in HFIR as mentioned in section 1.[20)]

The results of irradiation hardening in the high-irradiation-temperature region (740–800°C) were partly shown previously[13)] and the details will be published elsewhere,[20)] which show that the trend is slightly different from the data for 500–600°C. Irradiation hardening of pure W, W–3, 5Re and 10Re below 0.15 dpa at 740–800°C was almost the same as that at 500–600°C, as seen in Fig. 2, but the hardening of W–26Re was larger than that in the low-temperature region. With increasing dpa, the irradiation hardening of pure W and W–Re alloys at 500–600°C became larger than that at the 740–800°C temperature range. The mechanism based on microstructural observations will be discussed later.

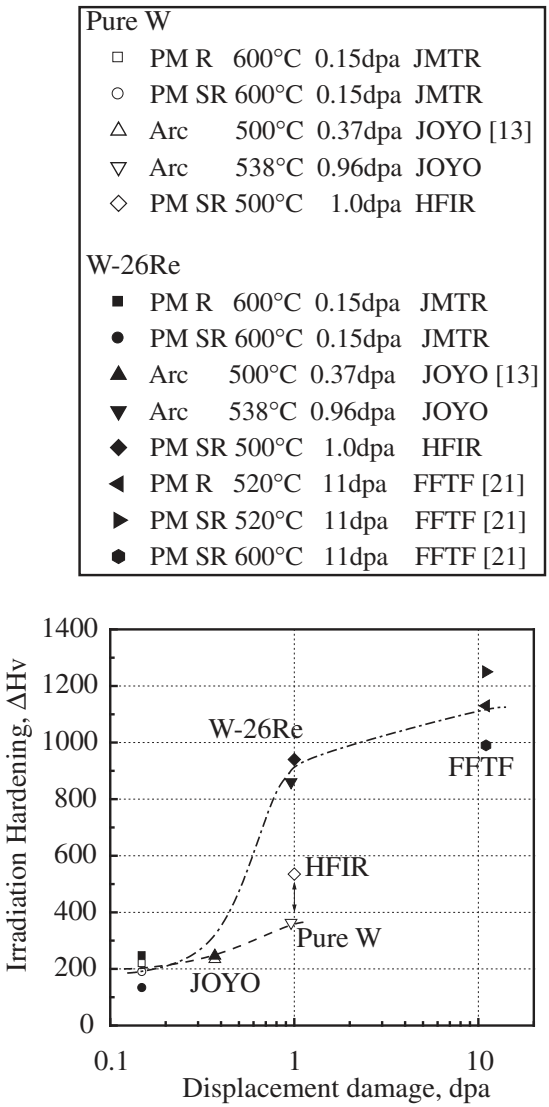

Fig. 3 Irradiation hardening of W and W–26Re after neutron irradiations between 500 and 600°C as a function of displacement damage.[16]

Figure 3 shows the irradiation hardening of W and W–26Re.[16] The irradiation hardening of W–26Re at the displacement damage from 0.1 to 1 dpa was significantly larger than that of W, and the irradiation hardening tended to saturate at approximately 1 to 10 dpa.[21] In the case of pure W, the irradiation hardening in the 0.1 dpa region was similar to that of W–26Re alloy, but it doubled after 1 dpa.[20] These hardening behaviors can be attributed to the difference in the microstructural evolution behaviors of W and W–26Re, as described in the next section.

4. Microstructure Development of Irradiated W and W–Re Alloys

The typical microstructures of irradiated pure W, W–5Re and W–26Re in the low-dpa region (dpa < 0.5 dpa) are summarized in Fig. 4.[15,17,19] The major defect clusters in pure W under these irradiation conditions were voids. Small amounts of loops were also observed. The void size and number density tended to decrease with increasing Re content, and the defect microstructures of 3, 5 and 10Re in this irradiation range were similar to that of W–5Re. Irradiation-induced precipitation was not confirmed in these specimens.

In the case of W–26Re, however, no void or loop but small needle like precipitates were observed. Diffraction patterns confirmed that the precipitates were symmetrically aligned along {100}. In addition, spherical precipitates were also observed. After 0.4 dpa irradiation at 740°C, longer needle like precipitates with high number density were clearly observed compared with that after 0.47 dpa irradiation at 583°C. The needle like precipitate was determined to be the χ phase (Re_3W).[10,14] These results agree with those of previous works,[10,11,18] obtained after high-dpa irradiation. The needle like precipitates were induced by the irradiation because the χ phase could not be formed in W–26Re under thermal equilibrium condition.

The microstructures of pure W and W–Re alloys under high-dpa irradiation are shown in Figs. 5 and 6. In pure W, void growth was observed, and the voids were found to arrange into an ordered void lattice, such that its axes were coincident with that of the host metal.[7,24] Figure 5 shows a typical image of the void lattice at low magnification.[13] These results agree with previous results for pure W.[5,8]

Figure 6 shows details of the microstructures of pure W, W–Re and W–Os alloys.[14,17] Needle like precipitates were observed in W–5Re and W–10Re alloys. In comparison with the pure W, smaller voids with a lower number density were also observed in W–5Re and W–10Re alloys.[13,14] In the case of the W–26Re alloy, no void and large precipitates with a high number density were observed after irradiation to 0.96 dpa at 538°C. In the case of W–Os alloys, no characteristic structure due to irradiation was observed in W–3Os after irradiation to 0.17 dpa at 400°C. However, needle like precipitates on the {110} plane were observed after irradiation to 1.54 dpa at 750°C. A few black dots but no void were observed.[14] The precipitate size was smaller than that in W–5Re alloy. These precipitates could not be identified from the diffraction patterns, but they are likely the σ phase (Os_xW_{1-x}, $x = 0.20$–0.35) because this is the only possible intermetallic compound according to the W–*y*Os phase diagram.[25]

No specific microstructure formed by the irradiation was observed by TEM in W–5Re–3Os after irradiation to 0.17 dpa at 400°C; however, the microstructure after irradiation to 1.54 dpa at 750°C included small needle like precipitates with a high number density, as shown in Fig. 5. This was similar to the microstructure observed in W–5Re irradiated under the same conditions. The observed plate or needle like precipitates on (110) along [110] were finer than those in W–5Re, and no voids were observed in the W–5Re–3Os alloys. It was also confirmed that the same precipitates were formed in W–25Re–3Os alloys irradiated to above 0.40 dpa at 750°C. These results suggest that over a few mass% Re or Os suppressed void formation and swelling. The number density of precipitates increased with increasing amount of these elements. The mechanism of the suppression effect was suggested by Herschits and Seidman.[11]

Rhenium is an undersized element in W; therefore, dumbbell-type interstitial clusters tend to form with Re atoms during irradiation. Williams *et al.* reported that the precipitates were found to have a WRe_3 composition of the χ-phase structure, and ReW of the σ phase structure.[10] The

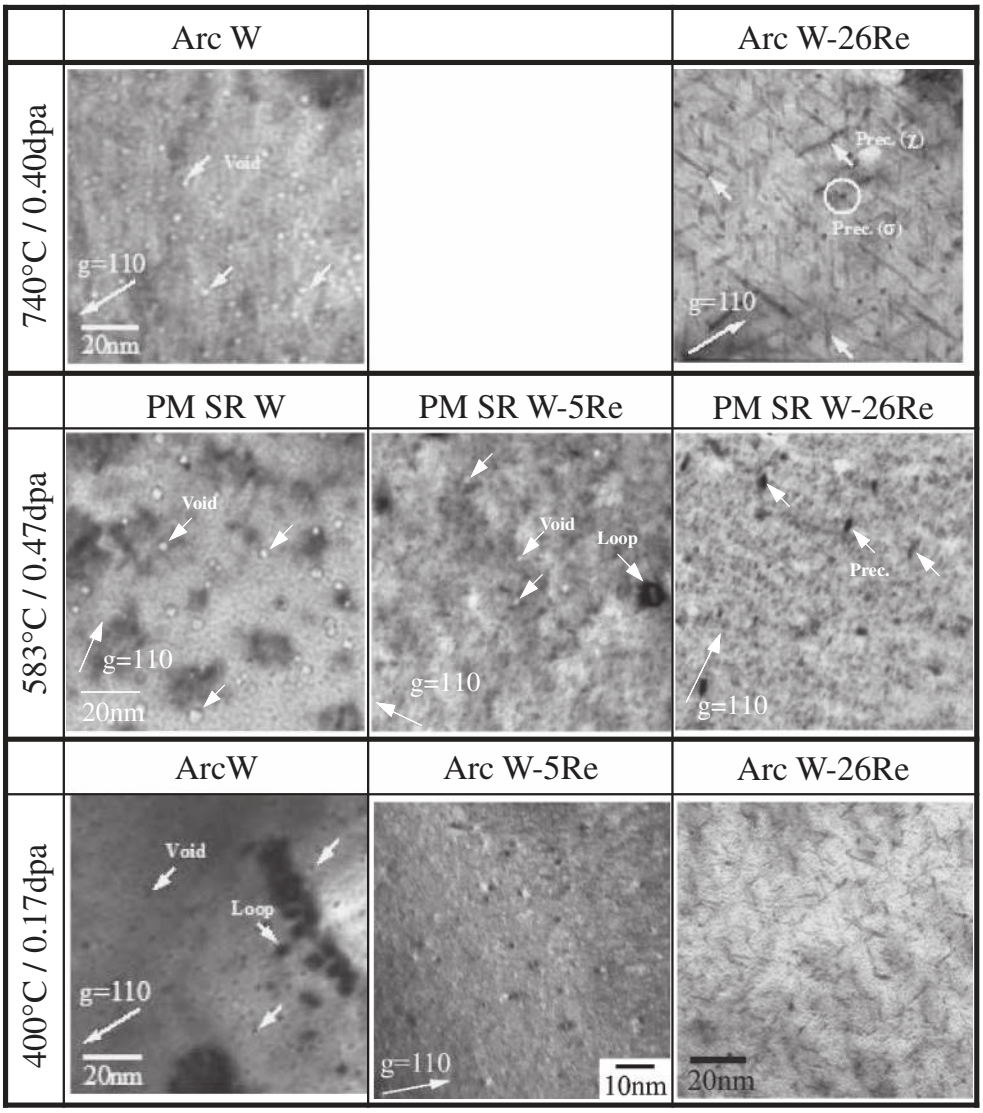

Fig. 4 TEM images of irradiated W and W–Re alloys after irradiations up to a low dpa level.[15,17,19)]

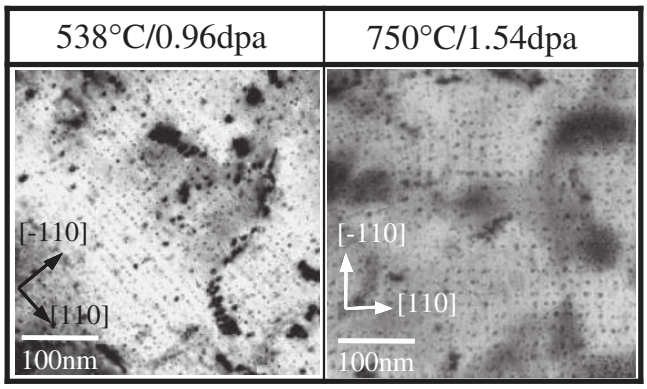

Fig. 5 TEM images of the void lattice in arc-melted W after neutron irradiations.[13)]

mechanism of the radiation induced formation of precipitates, WRe and WRe_3, was suggested by Herschits and Seidman.[11)] They concluded that homogeneous radiation-induced precipitation occurred in these alloys because these precipitates were not associated with either linear or planar defects or with any impurity atoms based on their works using an atom-probe field-ion microscope. A physical argument was presented for the nucleation of WRe and WRe_3 precipitates in the vicinity of a displacement cascade produced by primary knock-on atoms due to the interaction between self-interstitial atoms (SIAs) of W and di-Re clusters. They suggested that the strong bond between W and Re atoms likely plays a key role in the nucleation and growth of WRe clusters, and a plausible mechanism for the suppression of void swelling in W–Re alloys involved the dominance of vacancy SIA recombination. The strong recombination process between vacancies and SIAs trapped in immobile clusters involving SIAs and Re atoms prevented the accumulation of a sufficient number of vacancies for the nucleation and growth of voids.

Figure 7 summarizes the irradiation hardening data of W, W–Re and W–Os alloys combining the results of this work with those of previous works obtained by JOYO irradiation.[13,16)] Suppression of irradiation hardening by a small amount of Re addition (less than 5%) may be effective up to 1.5 dpa at 750°C. On the other hand, the W–26Re alloys showed significant hardening even after 1 dpa levels because of the significant irradiation-induced precipitation of σ (ReW) or χ (Re_3W) phase.[25)] The results of this work show that

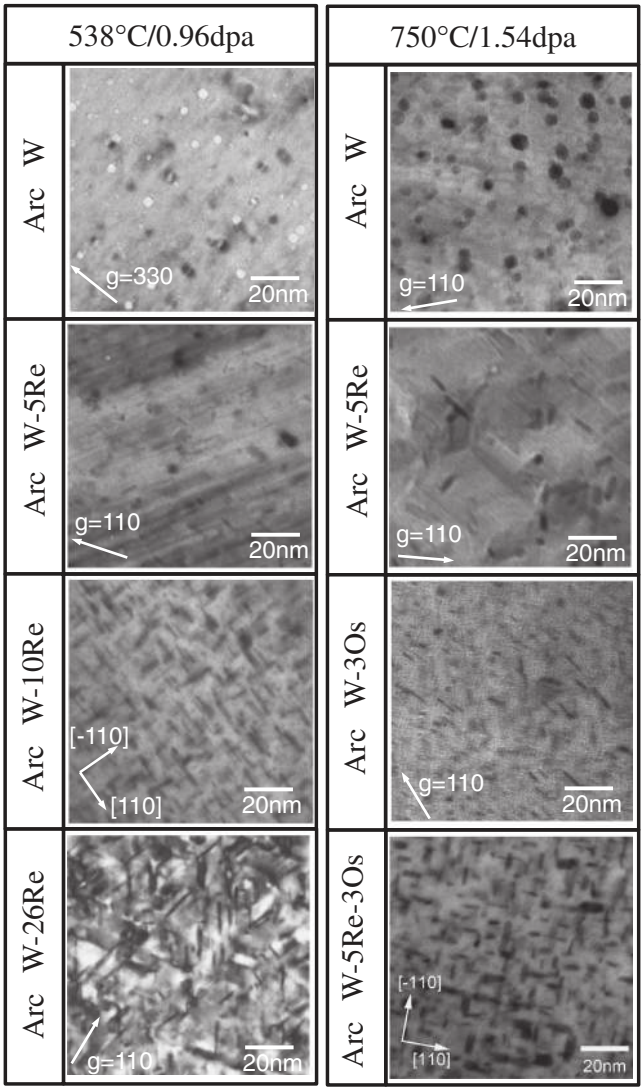

Fig. 6 TEM images of irradiated W and W–Re alloys after irradiations up to a high dpa level.[14,17)]

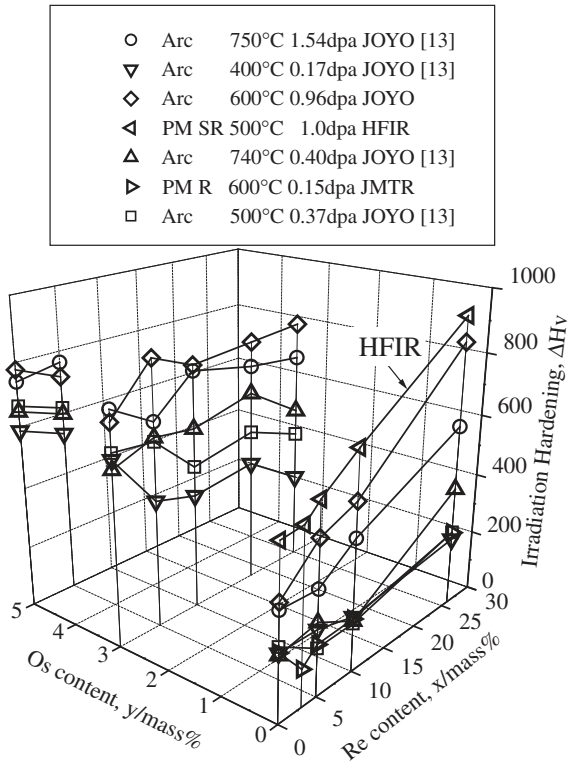

Fig. 7 Summary of irradiation hardening data for W–Re–Os alloys.[16)]

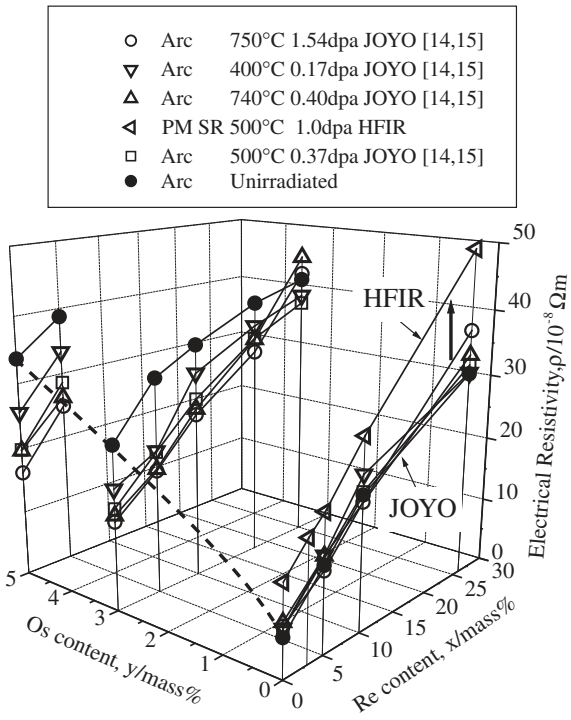

Fig. 8 Electrical resistivity of W–Re–Os alloys before and after irradiation.[16)]

irradiation hardening of W–Re alloys increases with increasing Re content, but the hardening may saturate when the precipitate structure well develops above 1.54 dpa and 750°C, respectively.

In W–3Os irradiated to 1.54 dpa at 750°C, there were a number of precipitates and black dots, but voids were scarcely observed. Thus, it is considered that the void suppression effect of Os is stronger than that of Re, and Os may enhance the formation of black dots such as interstitial defect clusters.

5. Electrical Resistivity and Effects of Solute Atom

Figure 8 shows the electrical resistivity of the W–Re–Os alloys after neutron irradiation under different conditions with our previous results on W–Re and W–Os alloys.[14,15)] In the case of the JOYO irradiation, no significant change in the electrical resistivity was observed in the W–Re alloys, while a decrease in the resistivity was observed in W–Os and W–Re–Os alloys after the irradiations. It is well known that an increase in the resistivity is due to an increase in the concentration of solutes. In the case of HFIR irradiation, the increase in electrical resistivity is larger than that in the case of JOYO irradiation, suggesting a higher transmutation rate of Re in HFIR irradiation than that in JOYO.

6. Discussion

Microstructural observations showed that irradiation-induced precipitates were formed in W–Re above a threshold

neutron irradiation fluence, which depended on the Re content, and as a resultant precipitation hardening occurred. Furthermore, the void lattice structure is formed above 1 dpa and may suppress void swelling. However, under fusion reactor conditions, the concentration of transmutation products will markedly increase in the matrix as the neutron fluence increases. The formation of irradiation microstructures, such as voids or void lattices, depends on the Re concentration in W, which has a high binding energy to vacancies in W. This also affects material properties, such as thermal conductivity and electrical resistivity. The solute element concetration in the matrix is decreased by precipitation and increased by nuclear transmutation, and then dynamic solute concentration balance without precipitates under irradiation is important to develop the irradiation resistant material. The data obtained with the W–Re–Os alloys to simulate transmutation effects also contribute to the investigation of the solute element effects.

On the basis of the results obtained so far, the microstructural changes in W by neutron irradiation can be predicted. In pure W, voids are formed at the early stage of irradiation and the void lattice structure appears at around 1 dpa at 500–800°C. This structure is expected to be stable up to several dpa. With increasing neutron fluence up to above 10 dpa, the concentration of transmuted Re increases to several mass%, and the balance between point defect production and annihilation in the void lattice structure changes so that the voids might shrink and precipitates are formed in the W matrix. The threshold concentration level of Re from in-solution to precipitation dominant level might be about several mass%.

In the case of W–26Re with a high Re content, no voids and loops are formed but rather needle like precipitates are formed at the early stage of irradiation. With increasing neutron fluence, highly dense precipitates appear, accompanied by severe irradiation hardening. On the basis of our data, it is expected that the addition of a small amount of Re suppresses void formation and hardening at the early stage of irradiation, which is considered to be due to the enhancement of defect recombination by the Re-interstitial cluster.

On the other hand, Re reduces the thermal conductivity of W, and the reduction rate per Re content is steep up to 5% Re compared with the alloys with higher Re content.[26] The thermal conductivity of W–2% Re is 30–40% less than that of pure W, although the degradation of thermal conductivity during reactor operation is expected to be moderate. Rhenium is a rare and expensive element but it is a major transmutation element of W, and it is produced and accumulates in W up to 6% during reactor operation after 30 dpa.[2] Therefore optimization of the Re addition is required to improve the radiation resistance of W. This might be in the range of 1 to 3%, although further experimental works are required for a more accurate estimation.

7. Summary

To understand the irradiation response of W in a fusion reactor, irradiation effects on hardening, microstructure development and electric resistivity of pure W and W–Re–Os alloys are studied after irradiation to 0.15 to 1.54 dpa at 400 to 800°C using fission reactors. In the low-dpa region (<0.4 dpa), irradiation hardening was suppressed by Re addition, but significant hardening appeared in W–26Re alloy in high-dpa (>1 dpa) region. The large hardening was caused by the irradiation-induced precipitation of WRe (σ–phase) and WRe_3 (χ–phase). Os was more effective for the irradiation hardening than Re owing to the precipitate formation. On the basis of these results, the alloy design of W for fusion reactor applications is suggested.

Acknowledgements

Post-irradiation experiments (PIE) were carried out at the International Research Center for Nuclear Materials Science of IMR Tohoku University and the Laboratory of Alpha-ray Emitters of IMR. The authors thank Mr. M. Narui, Mr. M. Yamazaki and the IMR staff for support of the PIE.

REFERENCES

1) H. Bolt, V. Barabash, G. Federici, J. Linke, A. Loarte, J. Roth and K. Sato: J. Nucl. Mater. **307–311** (2002) 43–52.
2) H. Bolt, V. Barabash, W. Krauss, J. Linke, R. Neu, S. Suzuki, N. Yoshida and ASDEX Upgrade Team: J. Nucl. Mater. **329–333** (2004) 66–73.
3) R. Neu *et al.*: J. Nucl. Mater. **363–365** (2007) 52–59.
4) T. Noda, M. Fujita and M. Okada: J. Nucl. Mater. **258–263** (1998) 934–939.
5) R. C. Rau, R. L. Ladd and J. Moteff: J. Nucl. Mater. **33** (1969) 324–327.
6) L. K. Keys and J. Moteff: J. Nucl. Mater. **34** (1970) 260–280.
7) V. K. Sikka and J. Moteff: J. Appl. Phys. **43** (1972) 4942–4944.
8) V. K. Sikka and J. Moteff: J. Nucl. Mater. **46** (1973) 217–219.
9) J. Matolich, H. Nahm and J. Moteff: Scr. Metall. **8** (1974) 837–841.
10) R. K. Williams, F. W. Wiffen, J. Bentley and J. O. Stiegler: Metall. Trans. A **14** (1983) 655–666.
11) R. Herschitz and D. N. Seidman: Nucl. Instrum. Methods Phys. Res. B **7–8** (1985) 137–142.
12) J. C. He, G. Y. Tang, A. Hasegawa and K. Abe: Nucl. Fusion **46** (2006) 877–883.
13) T. Tanno, A. Hasegawa, J. C. He, M. Fujiwara, S. Nogami, M. Satou, T. Shishido and K. Abe: Mater. Trans. **48** (2007) 2399–2402.
14) T. Tanno, A. Hasegawa, M. Fujiwara, J. C. He, S. Nogami, M. Satou, T. Shishido and K. Abe: Mater. Trans. **49** (2008) 2259–2264.
15) T. Tanno, A. Hasegawa, J. C. He, M. Fujiwara, S. Nogami, M. Satou, K. Abe and T. Shishido: J. Nucl. Mater. **386–388** (2009) 218–221.
16) A. Hasegawa, T. Tanno, S. Nogami and M. Satou: J. Nucl. Mater. **417** (2011) 491–494.
17) T. Tanno, M. Fukuda, S. Nogami and A. Hasegawa: Mater. Trans. **52** (2011) 1447–1451.
18) Y. Nemoto, A. Hasegawa, M. Satou and K. Abe: J. Nucl. Mater. **283–287** (2000) 1144–1147.
19) M. Fukuda, T. Tanno, S. Nogami and A. Hasegawa: Mater. Trans. **53** (2012) 2145–2150.
20) A. Hasegawa: ICFRM-15 (2011) submitted.
21) K. Ueda: Doctoral Thesis, Tohoku University (1998).
22) J. C. He, A. Hasegawa, M. Fujiwara, M. Satou, T. Shishido and K. Abe: Mater. Trans. **45** (2004) 2657–2660.
23) A. Leach and D. J. Jones: Powder Metall. **10** (1967) 174–191.
24) K. Krishan: Radiat. Eff. **66** (1982) 121–155.
25) A. Taylor, B. J. Kagle and N. J. Doyle: J. Less-Common Met. **3** (1961) 333–347.
26) M. Fujitsuka, B. Tsuchiya, I. Mutou, T. Tanabe and T. Shikama: J. Nucl. Mater. **283–287** (2000) 1148–1151.